Heliyon 10 (2024) e33706

Contents lists available at ScienceDirect

Heliyon

journal homepage: www.cell.com/heliyon

Research article

Chinese traditional medicine DZGP beneficially affects gut microbiome, serum metabolites and recovery from rheumatoid arthritis through mediating NF-κB signaling pathway

Liming Zhao [a,b], Kai Zheng [c], Xiaolin Wan [d], Qiang Xiao [b], Lin Yuan [e], Chuanfang Wu [a,**], Jinku Bao [a,*]

[a] Key Laboratory of Bio-Resource and Eco-Environment of Ministry of Education, College of Life Sciences, Sichuan University, Chengdu, 610065, Sichuan, China
[b] Hubei Key Laboratory of Biological Resources Protection and Utilization, Hubei Minzu University, 445000, Enshi, China
[c] Forest Seedlings and Wildlife Protection Management Station of Enshi Tujia and Miao Autonomous Prefecture, 445000, Enshi, China
[d] College of Forestry and Horticulture, Hubei Minzu University, 445000, Enshi, China
[e] Hubei Provincial Key Laboratory of Occurrence and Intervention of Rheumatic Diseases, Hubei Minzu University, 445000, Enshi, China

ARTICLE INFO

Keywords:
Transcriptome
16S ribosomal RNA
Mass spectrometry
Fecal microbiome
Traditional Chinese medicine
NF-κB pathway

ABSTRACT

Rheumatoid arthritis (RA) is globally treated with several commercially available anti-inflammatory and analgesic drugs, which pose adverse side effects in many cases. Due to increasing population affected by autoimmune disorder of joints inflammation, it is crucial to use natural therapies, which are less toxic at metabolic level and promote gut health. In this study, we investigated the potential role of a locally developed traditional Chinese medicine (TCM), namely Duzheng tablet (DZGP) in controlling the RA. For this purpose, we introduced RA in male mice and divided them into 5 different groups. High throughput transcriptome analysis of synovial cells after DZGP treatment in arthritic mice revealed a significant alteration of gene expression. The correlation analysis of transcriptome with metabolites revealed that DZGP specifically targeted the B cells mediated immunity pathways. Treatment with DZGP inhibited the cytokines production, while reducing the production of inflammatory TNF-α, which led to the alleviation of inflammatory response in arthritic mice. Additionally, we applied integrated approach using 16S rDNA sequencing to understand the microbial population in relation to metabolites accumulation. The results showed that DZGP promoted the healthy gut microbiota by maintaining the ratio of Firmicutes and Bacteroidota and introduction of two additional phyla namely, Verrucomicrobiota and Cyanobacteria. Therefore, it is concluded that DZGP offers an advantage over commercial drug by changing the metabolic profile, gut microbiota while exhibiting lower cellular toxicity.

1. Introduction

Rheumatoid arthritis is a very destructive and chronic autoimmune disease that generally manifests as systematic swelling of the joints. The initial manifestation of the disease is characterized by symmetrical peripheral joint damage. In later stages, the disease

* Corresponding author.
** Corresponding author.
E-mail addresses: wuchuanfang@scu.edu.cn (C. Wu), baojinku@scu.edu.cn (J. Bao).

https://doi.org/10.1016/j.heliyon.2024.e33706
Received 21 January 2024; Received in revised form 22 June 2024; Accepted 25 June 2024
Available online 26 June 2024

systemically affects organs such as the heart, muscles, lungs, and sometimes blood vessels, which can lead to rheumatoid vasculitis. Like many other autoimmune diseases, RA is more common in women [1]. Prolonged RA can damage the joints, leading to joint replacement surgery or premature death [2]. The complications caused by RA are not only serious health problems but can also have a huge financial impact [3,4]. Initially, rheumatoid arthritis was considered a non-fatal disease. However, increasing evidences suggest that patients with chronic RA have a short life expectancy [5–7]. Although patients in old age are more prone to RA disease, recent evidences suggest its prevalence in the juvenile stage [8]. As the course of RA prolongs, bacterial infection increases, which can eventually lead to premature death. There is also a consensus that drugs used to treat mild RA can cause a toxic reaction in the body [9].

Due to the autoimmune nature of RA, immune response-related B cells and T cells play a critical role in its pathogenesis. The immune-related cells can circulate in the blood or reside on the inner surface of synovial membranes. In RA disease, T cells activate fibroblasts or macrophages to convert them into tissue-damaging cells. In contrast, B cells play a risky role in the pathogenesis of RA (Bugatti et al., 2014). B cells support RA by secreting rheumatoid factors (RFs), pro-inflammatory cytokines, and anti-citrullinated protein antibodies (ACPAs) [10,11]. In addition to T and B cells, macrophages play a perilous role in the development of RA [12]. There is evidence that synovial macrophages show a high level of impaired ratio between inflammatory and anti-inflammatory macrophages in RA [13,14]. Analysis of joint synovial fluid in RA patients showed the presence of a high population of bone marrow macrophages (CD14++, $CD68^{+}$ and $CD16^{+}$), suggesting their cytokine-related inflammatory role in disease progression [15]. Treatment of RA patients with disease-modifying anti-rheumatic drugs (DMRADs), such as sodium aurothimalate (SAT), results in a decreased population of macrophages in synovial fluids. Therefore, it is clear that a decrease in synovial macrophages is associated with clinical improvement in RA patients [16,17].

In healthy tissues, synovial fibroblasts (SFs) provide the joint cavity with nourishing and lubricating molecules. RA studies in the mouse model suggest that the proliferation of synovial cells and their attachment to joints can lead to inflammation [18]. It is a well-established fact that synovial cell proliferation in particular, together with inflammation, can lead to joint damage [19]. As the synovial tissue proliferates, it extends over the articular cartilage and into the subchondral bone. Eventually, all of the affected joints are damaged.

Rheumatoid arthritis is very common in China [20]. Several surveys have shown that the incidence rate of RA ranges between 11.6 and 46.4 %, depending on the location and age group of people. The major challenges in the treatment of RA are the high cost and adverse effects of DMRAD. However, newer biological agents such as tumor necrosis factor-alpha (TNF-α) and interleukin-6 (IL-6) inhibitors have expanded the treatment options for RA. Due to the high cost and irreversible side effects, there is a great demand for alternative treatments. Traditional Chinese medicine contains a wide range of important chemicals with therapeutic and nutritional value [21].

In China, RA patients can be divided into several subgroups according to the nature of their syndrome. Several studies suggested that the choice of TCM is helpful in identifying biomarkers, gene networks, proteins and reactions of the human body at the biochemical level [22]. The approved TMCs such as Sinomenine (SIN) and Zushima Tablet (ZT) have been clinically used for RA treatment with positive results [23–25]. In recent years, a high correlation of gut microbiota with the development of inflammatory diseases such as RA has been observed. Indeed, gut microbes have a potential role in the exacerbation of RA. Studies have shown that the gut microbiota differs significantly between RA patients and healthy individuals. Certain bacterial species such as *Lactobacillus bifidus* are known to be associated with activation of IL17 + Th17 cells and Th1 cell responses that may play role in the exacerbation of RA [26]. The bacteria such as *Lactobacillus salivarius*, *Pseudomonas aeruginosa* and *Haemophilus* can be detected in the early development of RA and lead to metabolic disorders [27]. In this study, we used Duzheng tablet obtained from Hubei Province Pharmaceutical Preparation No. Z20210135, originating from the Tujia ethnic group in Enshi. Although, it is known to reduce swelling and relieve pain, but its effect on intestinal microbiota and metabolic activity has not been studied. In the present study we applied DZGP to collagen-induced arthritic (CIA) mouse model and conducted metabolic and transcriptomic analysis to deeply understand its effect at cellular and molecular levels.

2. Materials and methods

Selection of model and induction of arthritis: The purified immunogenic type II collagens were purchased from Chondrex Inc. (Cat#20021) and dissolved in 0.1 M acetic acid to a final concentration of 2 mg/ml [28,29]. Briefly, an emulsion containing 4 mg/ml Complete Freund's adjuvant along with *Mycobacterium tuberculosis* (collectively referred to as CFA, Chondrex Inc. Cat# 7009) was used to activate the immune cells [30]. After one week of adaptive feeding of the purchased rats, a blank group of rats was set aside and the remaining rats were used for further experiments. For initial immunization, we injected the emulsifier into the hind limbs and tail of the rats at three points with 100 μL per point. On the 7th day after the first immunization, we used immune-enhancing emulsifiers and repeated the previous operation to enhance immunity. Seven days after the second immunization, we evaluated the inflammatory status of the ankle and toes based on the criteria of four (0, 1, 2, 3, and 4) points [31]. 0 point: Appearance of toes was normal or without inflammation; 1 point: Mild redness and swelling of the toes; 2 points: Severely swollen toes; 3 points: indicates that all feet below the ankle are red and swollen; 4 points: Severe redness and swelling of the knee and ankle joints, even deformity. The left and right hind legs of the rat were scored separately, and the sum of the two hind legs reaching four points indicated successful modeling.

The highly CIA susceptible male Sprague-Dawley (SD) rats were selected for induction of arthritis. Twelve-week- old male SD rats were housed in 5 groups (6 rats in each group) and were maintained at 25 °C with 12-h light/dark cycle. These 5 groups were designated as, blank group (healthy mouse-designated as FK), arthritic mouse without any dose (CIA model designated as FX), arthritic mouse with commercial Methotrexate (MTX) treatment (1.05 mg/kg/d), low dose group (Duzheng DZGP-drug: 227 mg/kg/d) and

high dose group (DZGP drug: 908 mg/kg/d), respectively. The mice were purchased from Lianoin Changsheng Biotechnology Co., Ltd (License number, 2020-0001). Thirty mice (6-8 week-old) were intradermally immunized at the base of tail with 100 μg of mouse type-II collagen as described previously (Gasteiger et al., 2005). The onset of arthritis was daily observed by measuring the thickness of affected hind paw with microcalipers (Kroeplin GmbH, Schlüchtern, Germany). For transcriptomic and metabolomic assessment, the arthritic mice were sacrificed after four weeks of drugs treatment. For non-target metabolomic analysis, the blood serum was collected from the vena cava, while synovial tissues from the hind limb knee joint were excised for RNA extraction and further transcriptome analysis.

RNA Isolation, cDNA synthesis and transcriptome analysis: Total RNA from synovial tissues was extracted using commercial kit as recommended by the manufacturer (TIANGEN, Beijing China, CAT # DP424). For transcriptome synthesis, 100 ng of total RNA was used for library construction using NEBNext Ultra II Directional RNA Library Prep Kit. The libraries were paired-end sequenced on NovaSeq using the NovaSeq Reagent Kit (200 cycles). The sequencing data was checked for its quality using FastQC (Version 0.11.5) software [http://www.bioinformatics.bbsrc.ac.uk/projects/fastqc]. A raw sequence matrix for each gene was generated using featureCounts [32]. Unwanted variation in the sequencing data was determined using RUVseq [33]. The differential gene expression was estimated using edgeR software [34]. In total more than 20,000 transcripts for each combination was identified (Supplementary file-1). After filtration, the analysis was limited for total genes ranging from 800 to 1000 per sample (Supplementary file-2). While, the KEGG enrichment analysis was conducted for approximately 200 transcripts in each case (Supplementary file-3). The heatmaps for transcriptomics data were generated using heatmap-2 function integrated into R package.

Extraction and analysis of non-target serum metabolites: Blood serum was collected from the inferior vena cava, through a coagulation promoting tube. The tubes were labeled and centrifuged at 3000 rpm for 10 min. The supernatant (serum) was separated and stored at −80 °C for further processing. For each 50 μl of serum sample, 300 μl of extraction solution was added (CAN: Methanol = 1:4, V/V) containing internal standards. The mixture was vortexed for 3 min and centrifuged at 12,000 rpm for 10 min to extract the small molecules. The supernatant was transferred to a new tube and stored at −20 °C for 30 min and then centrifuged at 12,000 rpm for 10 min. About 180 μL supernatant was transferred for LC-MS analysis. The original LC-MS data was converted into mzML format by ProteoWizard software [35]. Principal component analysis (PCA) was performed on samples including quality control samples (QC samples) by using R software. In order to perform the differential metabolite screening in the metabolome data, both univariate and multivariate statistical analyses were performed. Multivariate analysis included PCA and Orthogonal Partial Least Square-Discriminant Analysis (OPLS-DA). Differential metabolites screening was assessed with the *P*-value or FC values. Kyoto Encyclopedia of Genes and Genomes database (KEGG) was used for identification and enrichment of the metabolic pathways [36].

DNA extraction, PCR amplification and metagenomic analysis of 16S rRNA genes: For 16S rRNA analysis, the cecal segment of intestine was excised and stored at −80 °C till further use [37]. Microbial DNA extraction from cecal samples was performed using PowerSoil DNA extraction kit (MoBio Carlsbad, CA, USA). Briefly, the frozen cecal samples were first treated as described earlier [38]. The pretreated samples in tubes were homogenized for 1 min, three times with 1-min rest period (BenchTop homogenized, MP Biomedicals, Santa Ana, CA, USA). DNA concentration was measured with Nanodrop (nanodrop-2000- Thermo Scientific, Waltham, MA, USA). For broad-taxonomic amplification of 16S-rRNA genes, the specific primers were used as described earlier [39]. For PCR reactions, the Phusion high fidelity DNA polymerase (Thermo Scientific) was used in a standard 25 μl reaction. Approximately, 3 μg 16S specific primers were added into 50 ng of metagenomic DNA. The PCR reactions were run as follows: 94 °C for 30 s; 15 cycles of 94 °C for 10 s, 47 °C for 40 s and 72 °C for 60 s followed by a final extension at 72 °C for 10 min. The amplified PCR amplicons were further purified using bead base PCR purification kit on Qubit fluorometer (Qiagen, XX, Qubit 3.0 fluorometer). The purified PCR amplicons were quantified with Qubit dsDNA HS Assay Kit (Thermo Scientific) and visualized using agarose gel electrophoresis. The samples were prepared for sequencing according to the Illumina guidelines. The sequencing was done using Illumina NovaSeq platform [40].

Bioinformatic analysis of microbiome and metabolomic data: Metabolome detection and microbial amplicon sequencing were performed for all the samples, respectively. Subsequently, their correlation analysis was also performed on differential metabolites and differential bacterial species. Principal component analysis (PCA) was performed to visually observe the differences in metabolome and microbiome between sample groups. The PCA was performed using the prcomp function of R software (www.r-project.org, version 4.1.2). The primer sequences integrated into the sequenced files were removed and the raw data was filtered using CLEAN [41]. Based on the effective clean data, amplicon sequence variants (ASV) were generated. For each ASV sequence, the corresponding species information and the abundance distribution was obtained. ASV data was also used for phylogenetic tree construction and Operational Taxonomic Unit (OTU) identification. For OTU clustering, both Delbur and DADA2016 were implemented using QIIME2 [42,43]. Venn plot analysis was performed to obtain the species richness and evenness within a sample. The species abundance information with confidence from different samples was visualized through Krona tool [44]. The heat map was generated using the relative abundance of bacteria (Phylum, Class, Genera, Species levels) (www.heatmapper.ca/expression). Alpha and beta diversity analysis for total ASVs were carried out using the Unifrac distance, which calculates the distance between samples using evolutionary relationship between the samples [45,46]. The R software (v4.2.0) was used for principal component analysis (PCA) principal coordinate analysis (PCoA) and non-metric multidimensional calibration (NMDS). In order to look for the different species between groups at each taxonomic level (Phylum, Cl ass, Order, Family, Genus, Species), the T-test test was performed to find the species with significant difference (p-value$<$0.5). The Phyloseq (v4.2.0) package of R software (v1.40.0) was used to calculate the Unifrac distance and constructing the UGPMA. The unweighted pair group method with arithmetic means (UGPMA) was used to calculate the phylogenetic tree and diversity between alpha and beta groups. Spearman rank correlation analysis was used to describe the correlation between microbiome and metabolome. Correlation analysis was performed using the cor function of R software, and the significance test of correlation was calculated using the corPvalueStudent function of GCNA package of R software v4.2.0 [47]. Spearman correlation coefficients of microorganisms and metabolites were displayed through clustering heat map.

3. Results

Effect of DZGP and MTX on body weight of CIA rat model: All the rats were raised in animal rooms with constant temperature (20–25 °C). The CIA model group rats showed a significant decrease in activity compared to the normal group, preferring to gather in groups, with dull fur, lethargy, reduced food and water intake, slow or even reduced weight gain, swollen and deformed foot joints, and some rats had ulceration and difficulty in moving (Figure-S1). After treatment with DZGP and MTX, we compared the arthritic mouse with the control group (Fig. 1A–F). The mental state of the DZGP treated and MTX groups gradually improved. The foot joints of the high-dose DZGP group (908 mg/kg/d) and MTX group rats significantly recovered (Fig. 1A–F).

Transcriptome analysis revealed differential gene expression in RA induced rats: We performed RNA sequence analysis of synovial tissues to study gene expression in comparison to healthy, commercially available drug and DZGP treated arthritic mice. The transcriptome PCA analysis showed a separation of samples with the changing drug patterns (Fig. 2). The PCA analysis revealed a clear difference of samples between healthy group and other arthritic mice (Fig. 2). The healthy samples data clustered separately in the 2D PCA plots of transcriptome and metabolome, respectively (Fig. 2A and B), while the inflamed samples tended to cluster together. Interestingly, the difference of clusters can be observed for high dose of DZGP and other treatments. Indeed, the PCA analysis showed that high dose of DZGP significantly alters the transcriptome and metabolome profile in arthritic mice. Sequencing data for each treatment combination comprised of more than 20,000 genes, where more than 600 genes were differentially expressed (DEGs; Supplementary file-1). To characterize the cellular pathways and metabolites together, we performed a high throughput KEGG

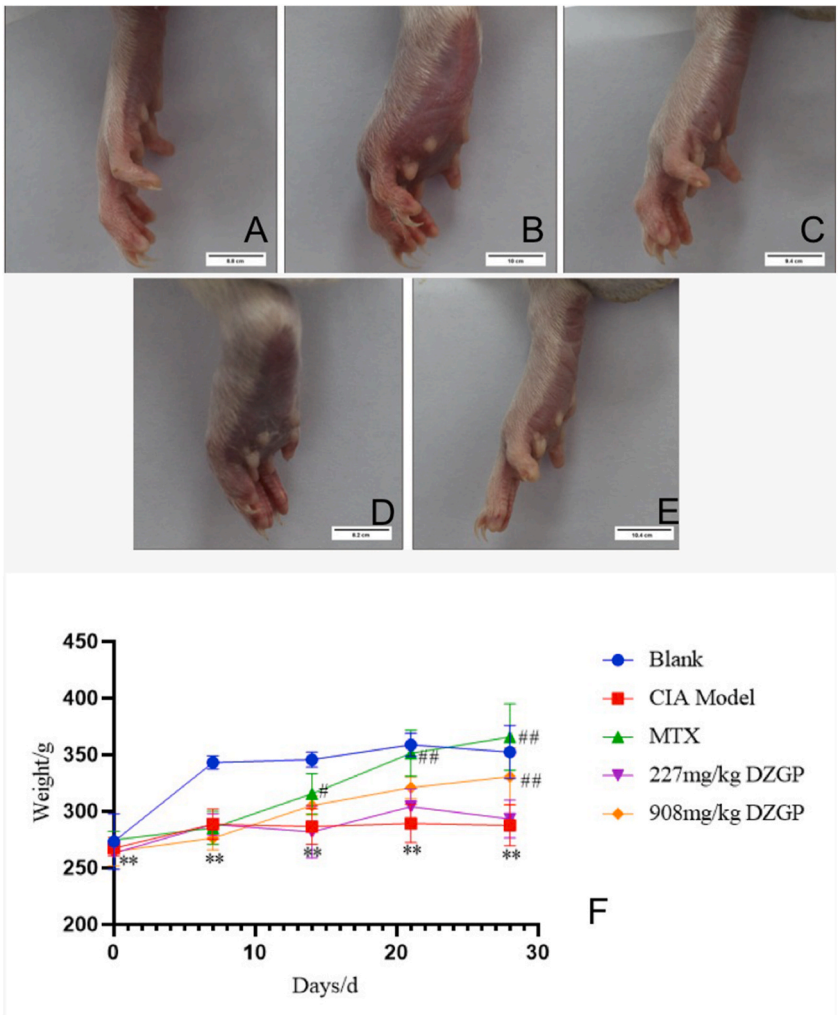

Fig. 1. Observation of DZGP impact on the general living status of CIA rat model. Panel-A represents the healthy or blank group. Panel-B represents the CIA model. Panel-C represents MTX treated arthritic mouse. Panels D and E represent the impact of 227 mg/kg and 908 mg/kg dosages of DZGP. A significant difference in weight gain between the CIA model group and the blank normal group was observed after 28 days of medication treatment (F). The weight of the blank normal group increased steadily, while the model arthritic group showed the slowest growth, with a decrease in body weight at one point.

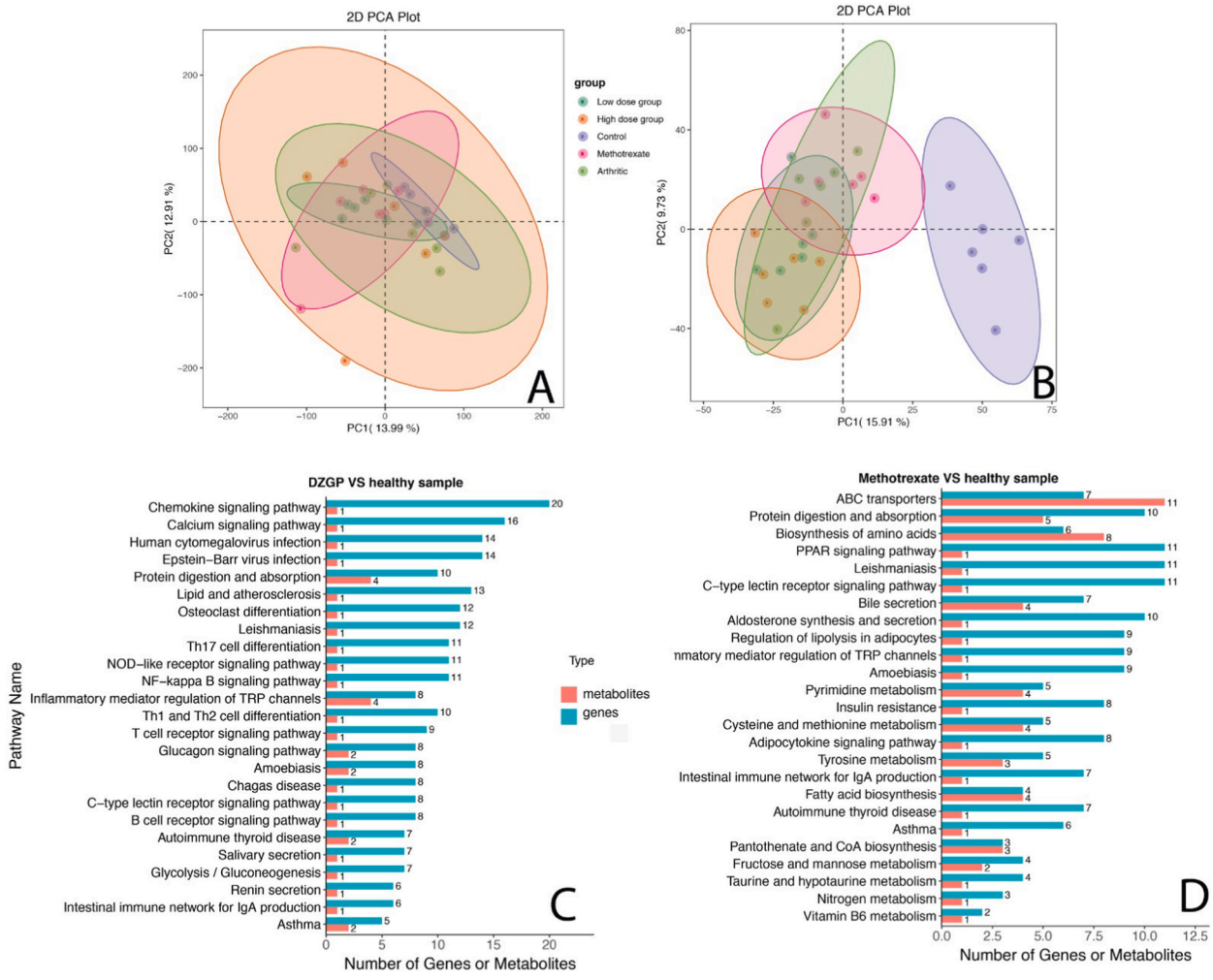

Fig. 2. Principal component analysis for transcriptome (A) and metabolome data (B): Metabolome and transcriptome correlation KEGG enrichment analysis for DZGP (C) and methotrexate treated mice (D).

enrichment analysis for each sample studied here (Fig. 2C and D).

The differential genes and metabolites expression analysis through KEGG enrichment of traditional DZGP medicine and commercially available drug (MTX) in comparison to healthy group of mice showed a significant difference between both the treatments. The KEGG enrichment analysis revealed that the DEGs in case of DZGP treatment were more enriched in chemokine signaling pathway as compared to commercial drug. By mapping the pathways, it was revealed that activation of chemokine signaling pathway resulted in up-regulation of Src, Rac, GRK and PLC genes, which help in cellular survival, growth and movement (Fig. 3).

Several other pathways like ABC transporter, fatty acids biosynthesis, protein digestion and absorption showed relatively increased transcripts expression in DZGP treated samples. However, from the available data, it was clear that DZGP specifically targeted the metabolic pathway, as their level did not increase despite of transcripts abundance. Most importantly, we identified the B cell receptor-signaling pathway, and NF-κB pathway, which showed increased transcripts expression level in case of DZGP treatment as compared to MTX (Fig. 3A and B). By mapping the B-cells receptor pathway, it was identified that several genes like PIR-B, FcgRIIB and LEU13 were up regulated. The detailed analysis also suggested that the genes related to Ig production (Rac and CARMA1) were also over-expressed, indicating their role in RA treatment through DZGP (Fig. 3). Interestingly, the correlation of metabolites and transcripts was completely different for both treatments. The correlation heatmap for both omics data revealed a significant difference between DZGP and methotexrate, indicating a different mode of action of both treatments (Fig. 4A and B). As a matter of fact, both treatments showed a quite unique and opposite patters of correlation for their transcripts and metabolites (Fig. 4A and B). In case of metabolomic data, it was observed that during treatment with methotexrate, the metabolites related to protein digestion and adsorption and minerals were increased. While the metabolites in case of DZGP treatment remained in constantly controlled quantity. It can be predicted from the current analysis that B cells mediated cell-signaling pathways and NF-κB pathways were specifically targeted by DZGP as their related metabolites levels remained significantly low.

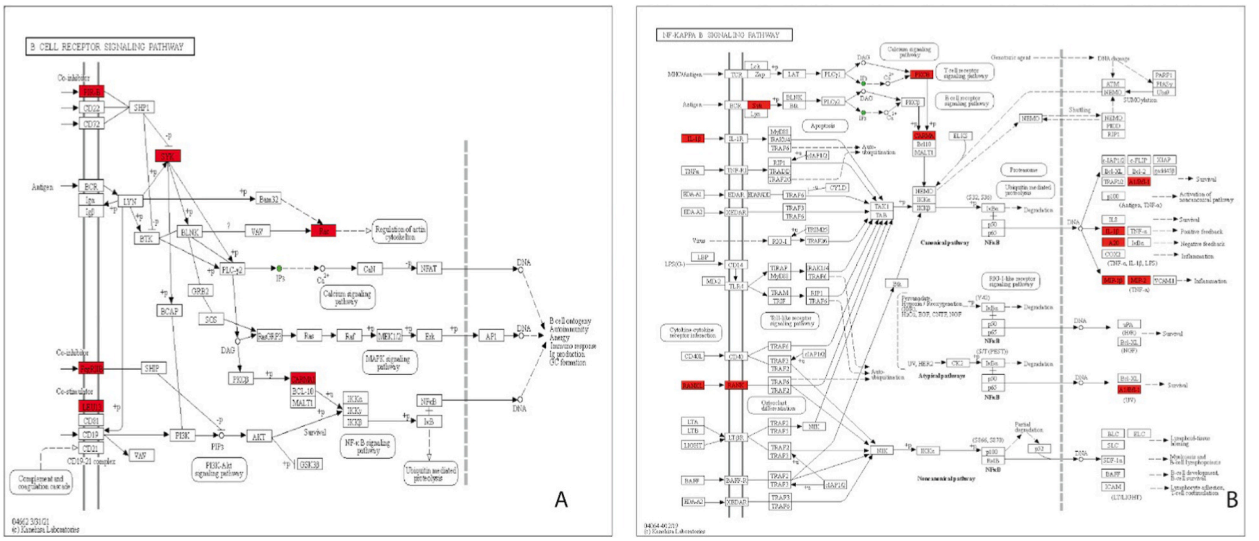

Fig. 3. The most important pathways identified through the KEGG enrichment analysis after treatment with DZGP drug. Panel –A shows the targeting of B cell receptor pathway, while Panel-B represents genes related to targeting of NF-κB pathway. The red boxes represent up-regulated genes.

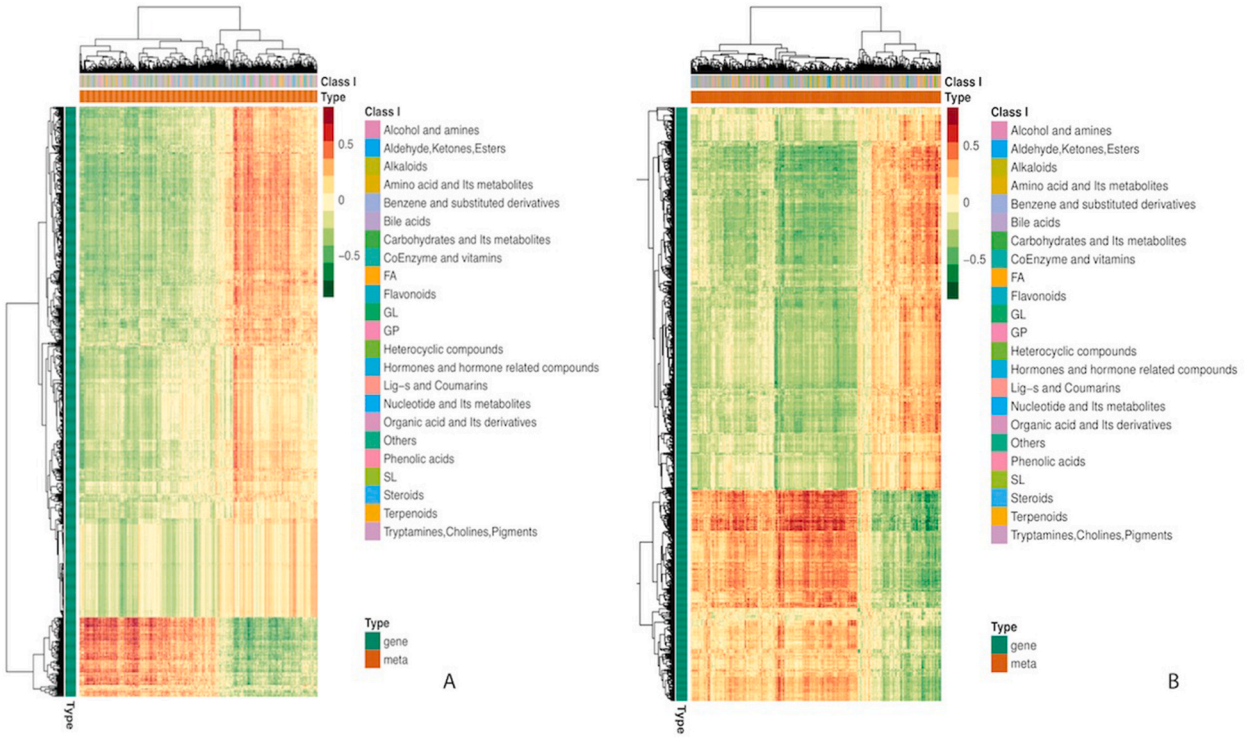

Fig. 4. Correlation heat map for transcriptomics and metabolomics data. Panel-A represents DZGP treated groups, where transcriptomes abundance is negatively correlated with metabolites, while panel-B represents the Methotrexate differential response.

Changes in species accumulation at individual and community level: High throughput sequencing of 16S rRNA genes revealed the alpha and beta diversity of microbial communities. The species richness and diversity analysis were confirmed through box plot and rarefaction curves (Fig. 5 A and B). The species accumulation box plot (Fig. 5A) flattened when number of samples reached 29, indicating the fact that OUT sequences were sufficient to predict the species richness of the samples. Similarly, the rarefaction curve tends to asymptotes, providing the adequate evidence of species richness and bacterial community diversity.

The beta diversity indexes were calculated using the principal coordinate analysis (PCoA) and cluster analysis method of weighted

unifrac UPGMA tree (Fig. 6). The control and RA samples were far apart from each other indicating a clear separation between the two groups (Fig. 6A). Likewise clear separation was found between DZGP and methotrexate treated samples. In addition, the UPGMA tree exhibited that high dose of DZGP and arthritic samples tend to cluster together (Fig. 6B).

Gut microbiota profile in response to DZGP treatment: To determine the difference between gut microbes of healthy, arthritic mice, methotrexate and DZGP treated mice; we compared the 16S rDNA sequences. UniFrac analysis suggested that microbiota of these 5 different groups were significantly different from each other. In total, 13,760 clean ASVs were generated and analyzed for diversity analysis at genus level (Supplementary file-4). We observed 35 different abundant taxa at different taxonomic levels (Supplementary file-5) and differentially abundant taxa at genus level are highlighted (Fig. 7).

As expected, samples from healthy mice showed enormous diversity and abundance in microbial population. However, the arthritic mice and the mice treated with methotrexate showed a significant drop in Acideobacteriota population (Fig. 8A). The data suggests that low dose of DZGP still supported relatively high diversity in microbial population in comparison to methotrexate and high dose of DZGP drugs. The phylum-level profiles for all the treated groups were very close to each other with few exceptions (Fig. 8B). In the control samples (no drug treatment), there was an increase in Acideobacteriota (Fig. 8B), which resulted in reduction of other microbial diversity. It can be observed from the data that structure of microbiota in methotrexate and DZGP treated mice was not similar. The methotrexate treated mice showed increased level of Firmicutes. Both methotrexate and control or healthy samples, showed an increase in the abundance of phylum Proteobacteria compared to healthy and RA samples (Fig. 8B). It can also be observed that population level of bacteria belonging to phylum Bacteroidota and Verrucomicrobiota increased significantly compared to control samples. On the other hand, bacteria belonging to phylum Proteobacteria were significantly reduced in the treated samples (Fig. 8B). Similarly, Euryarchaeota (methanogens) were also reduced in the drug treated samples (Supplementary file-6). The species annotation data was visualized using Krona analysis which demonstrated significant difference among the gut microbiota of treated and RA samples.

Metabolic and microbiome changes in mice after DZGP drug treatment: In addition to the changes in transcriptome and metabolome profiles of synovial fluid, we aimed to investigate how microbiome and metabolome are correlated. Therefore, plasma samples of treated and untreated CIA mice were analyzed using untargeted metabolomics approach. The LC-MS analysis detected 4909 metabolites. Several of the metabolites were altered in DZGP treated mice. Principal component analysis for metabolites revealed complete separation of control samples from arthritic samples (Fig. 9A). PCA analysis for microbial composition revealed the differences of control and treated samples at different taxonomic levels (Fig. 9B).

The differences among the groups for microbial population were filtered at various taxonomic levels. We identified 33 phyla, which were markedly different in abundance between the groups (Supplementary file-7). The relative abundance analysis at phylum level for each combination revealed that methotrexate treated mice had very fewer microbes (n = 4) as compared to control mice (Fig. 10A). Indeed, only four phyla, namely Euryarchaeota, Actinobacteria, Actinobacteriota and Cyanobacteria were differentially abundant in methotrexate treated arthritic mice. In case control groups, only 8 different phyla were found in abundance (Fig. 10B). While in DZGP treated group of arthritic mice, we observed 10 known phyla. These phyla included, Firmicutes, Bacteroidota, Verrucomicrobiota, Proteocacteria, Euryarchaeota, Actinobacteria, Actinobacteriota, Cyanobacteria and Fusobacteriota (Fig. 10C).

Whereas the Verrucomicrobiota and Cyanobacteria were in addition to 8 known phyla present in other groups of mice studied here. Both of these microbes mainly showed negative correlation with metabolites. To further determine the correlation between specific dominant bacteria associated with DZGP and other treatments, we used Pearson heatmap for dominant microbes with top-20 enriched metabolites. Interestingly, the types of top-20 metabolites accumulation in DZGP treated CIA mice were significantly changed in comparison to control and methotrexate treated mice. For example, Firmicutes did not show any correlation with Methylparaben

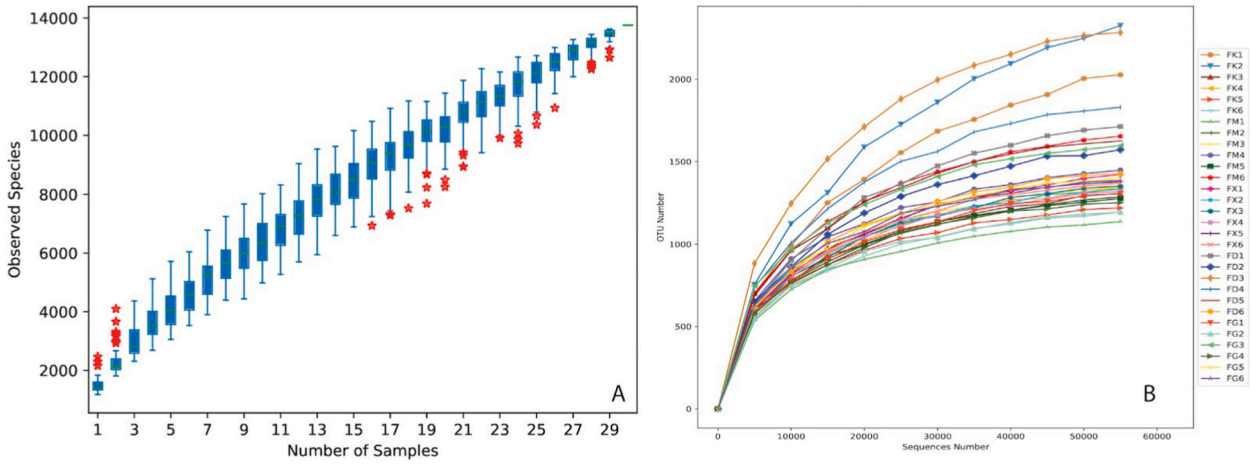

Fig. 5. Alpha diversity in control, arthritic and treated samples based on ASV. A- Species accumulation box plot, describing the species diversity with the increase in sample size. B- Species diversity curve, where FK, FX, FM, FD and FG represent the healthy, arthritic, MTX treated, low dose groups and high dose groups, respectively.

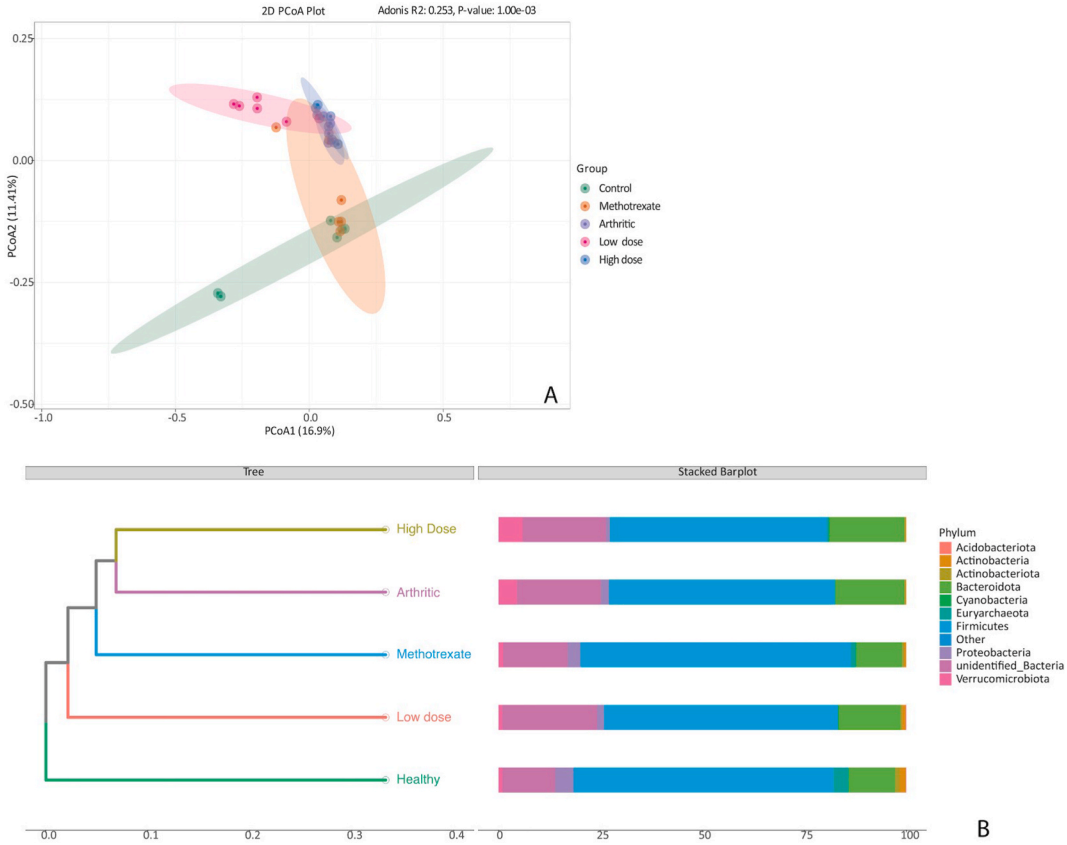

Fig. 6. Beta diversity index analysis. A- Principal coordinate weighted unifrac analysis. B- The UPGMA phylogenetic tree representing the distances with arithmetic means. The bars on right side indicate the microbial richness at phylum level.

metabolite in control mice, while in case of DZGP Firmicutes showed a positive correlation with Methylparaben (Fig. 10C).

4. Discussion

Traditional Chinese medicines have been proven to be very effective to treat several diseases and neutralize their toxic effects through different mixtures of herbs. Many TCM recipes have been used to treat RA [48]. In tradition, a microbial community habitat (microbiome) can be analyzed through metagnomic analysis. The inclusion of complete transcripts data (transcriptome) in relation to microbiome expands the significant implications of environmental factors associated with host response. In this study, we analyzed whether a locally used drug namely DZGP can modulate the RA-induced joints inflammation in relation to change in transcriptome, microbiome and metabolome. We specifically used CIA male SD rats that are highly susceptible to RA. We treated the RA affected mouse with two different doses (low and high) of a traditional DZGP, while MTX was used as a positive control in comparison to locally developed DZGP. MTX treatment has been widely used and its impact on microbiome and metabolome is well studied. However, DZGP mediated modulation of RA has not been investigated. Interestingly, DZGP even at moderate level reduced the RA pathogenesis, however main effects were observed at higher dose. Where DZGP reduced local and systemic inflammation, it also improved the gut microbiome and serum metabolome.

The TNF-α is a pleiotropic cytokine produced by many different types of cells in the body. However, cells of the monocytic lineage such as macrophages, astroglia, microglia, Langerhans cells, Kupffer cells, and alveolar macrophages, are the primary synthesizers of TNFα. Cytokine TNF-α has many effects on various cell types and has been identified as a major regulator of inflammatory responses and is known to be involved in the pathogenesis of some inflammatory and autoimmune diseases. Cytokines like TNF-α are overexpressed in RA affected joints and play a significant role in pathogenesis of arthritis [49]. B cells play a critical role in regulating immune cells and cytokine release [50]. It is an established fact that imbalance activities of cytokines favor the induction of joint chronic inflammation. Particularly, the tumor necrosis factor (TNF) has been proven to be important as a therapeutic target. Previous investigations have shown that MTX treatment is unable to reduce the TNF-α level in blood serum [48,51]. Our analysis suggests that DZGP treatment directly targets the B cell receptor-signaling pathway and controls the TNF-α accumulation in the synovial fluid. Any intervention to block TNF results in higher response of achieving clinical outcomes. In this study using DZGP as an RA treatment drug, the metabolomics study revealed a negative correlation between activation of NF-Kappa B (NF-κB) signaling pathway and

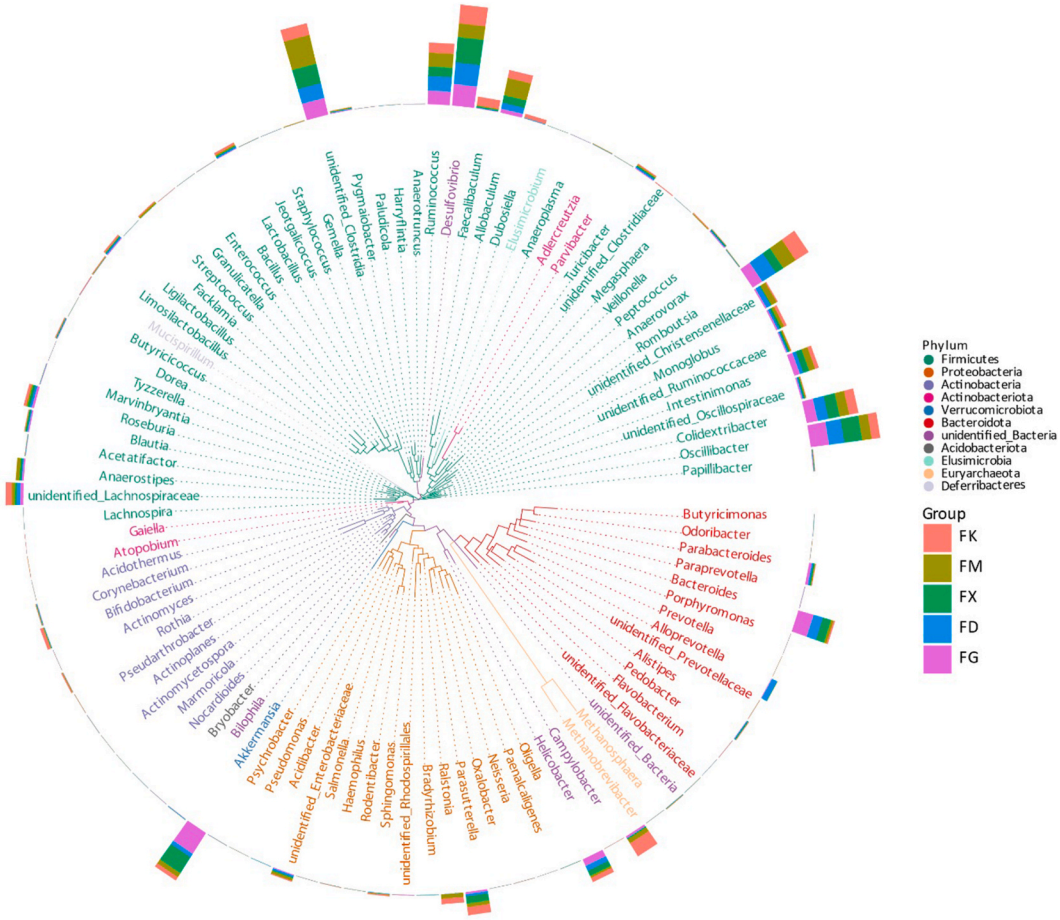

Fig. 7. Microbial diversity at genus level based on ASV sequences. Phylogenetic tree at genus level for microbes identified from 5 different groups of mice.

accumulation of its metabolites. The NF-κB are well-known transcription factors, which play a significant role as a regulator of inflammation in rheumatoid arthritis [52,53]. The over-expression of genes related to TNF and NF-κB is plausible due to pre-induction of RA. Nevertheless, relatively lower accumulation of their related metabolites suggests that treatment of DZGP plays an important role in targeting NF-κB accumulation. Although, MTX is a well-known gold standard medicine to down-regulate RA induced inflammatory response in human [54]. However, in agreement with other studies, MTX changed the metabolic profile by alterations in ABC transport pathway, amino acid and lipid metabolism [55]. Interestingly, DZGP treatment showed a quite different response in comparison to MTX treatment. The DZGP significantly targeted the protein and lipid metabolism pathway and balanced their accumulation at cellular level. These findings suggest that DZGP treatment is better than MTX at clinical level.

The individuals treated with different drugs showed altered metabolism and sometimes may lead to organ failure [56]. Changes in gut microbiome promoted by different drugs can also alter the immune response. It has been established that MTX use can lead to hepatotoxicity [57], however, the possible association between gut microbiome changes and the metabolic shifts influenced by DZGP were unknown. The correlation data on combination of microbiome and metabolome was very instrumental in understanding the treatment mechanism. Different microbes showed a range of positive and negative correlation with metabolites. Our results are in agreement with the previous findings that anti RA drugs can cause a significant change in certain microbes. For example, the Firmicutes phylum is a main component of gut microbiome. However, its increased abundance is associated with several adverse functions of liver functions [58]. Additionally, the ratio of Firmicutes and Bacteroidota is very important in RA induction [59]. In our analysis, high dose of DZGP resulted in significant reduction of Firmicutes while a relative increase in Bacteroidota was observed. These observations indicate that DZGP can be less toxic to liver cells as compared to MTX. Furthermore, a high positive correlation was observed between Firmicutes and methylparaben metabolite. The methylparaben is a well-known anti-microbial preservative, which can have potential implications in population reduction of Firmicutes as compared to control samples.

Presence of Cyanobacteria phylum in DZGP treated samples is another interesting finding in our omics analysis. Cyanobacteria (blue-green algae) are generally consumed as a source of nutrients to promote health and have pharmaceutical value [60]. The unique presence of Verrucomicrobiota in the DZGP treated samples indicates its potential to regulate the immunity [61]. The member species

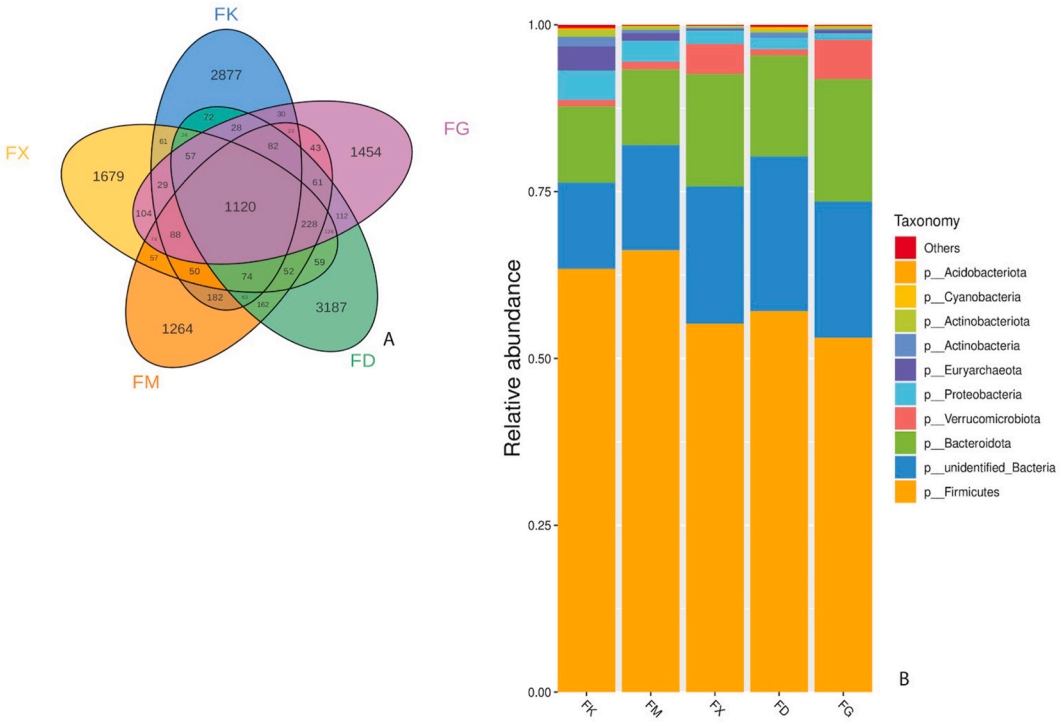

Fig. 8. A- Venn diagram of ASV sequences from 5 different groups of mice. B- relative abundance of top 10 bacteria phyla. The methotrexate treated samples showed high level of Firmicutes (sample FM) as compared to other treatments.

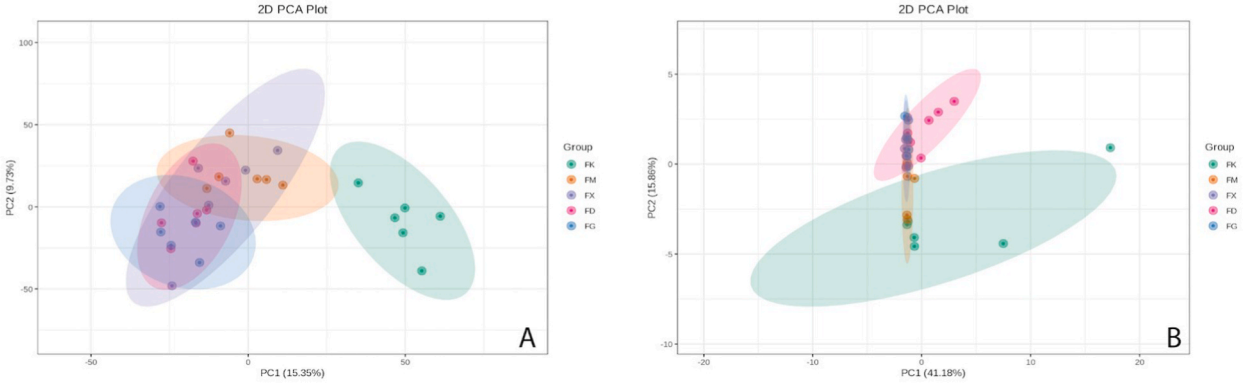

Fig. 9. Differential metabolites and microbiota profiling over RA treatment. A- Principal component analysis of control over arthritic samples in relation to differential metabolites accumulation showed significant variation. Samples on right represent the healthy samples. While, the samples on left side represent RA samples with variations in different types of treatments. B- Microbial profile of healthy (bottom) and arthritic samples with different treatments.

of phylum Verrucomicrobiota are known to degrade the sulfated polysaccharides and play an important role in carbon cycling [62]. However, we also observed that Verrucomicrobiota phylum was not associated with top-20 metabolites. Given the importance of Cyanobacteria and Verrucomicrobiota as a gut microbe, it can be concluded that DZGP has pronounced effects on the maintenance of beneficial bacterial population. Various mechanisms of Chinese herbal medicine in treating infectious diseases have been explained. These include antibacterial (i.e., inhibition of bacterial growth and inhibit formation of bacterial biofilm) as well as antiviral effects (i.e., suppress replication and induce cell apoptosis). Apoptosis is the process of programmed cell death, which helps to eliminate cells that are not required. Other mechanisms of Chinese herbal medicine are the antioxidant effect (reduce free radicals) and anti-inflammatory ability that prevent or inhibit the release of inflammatory mediators, cytokines, and other factors that are generated during the inflammatory response. Challenges, prospects, and potential applications of TCM are extensively studied due to its activity, safety, and the long history of clinical application.

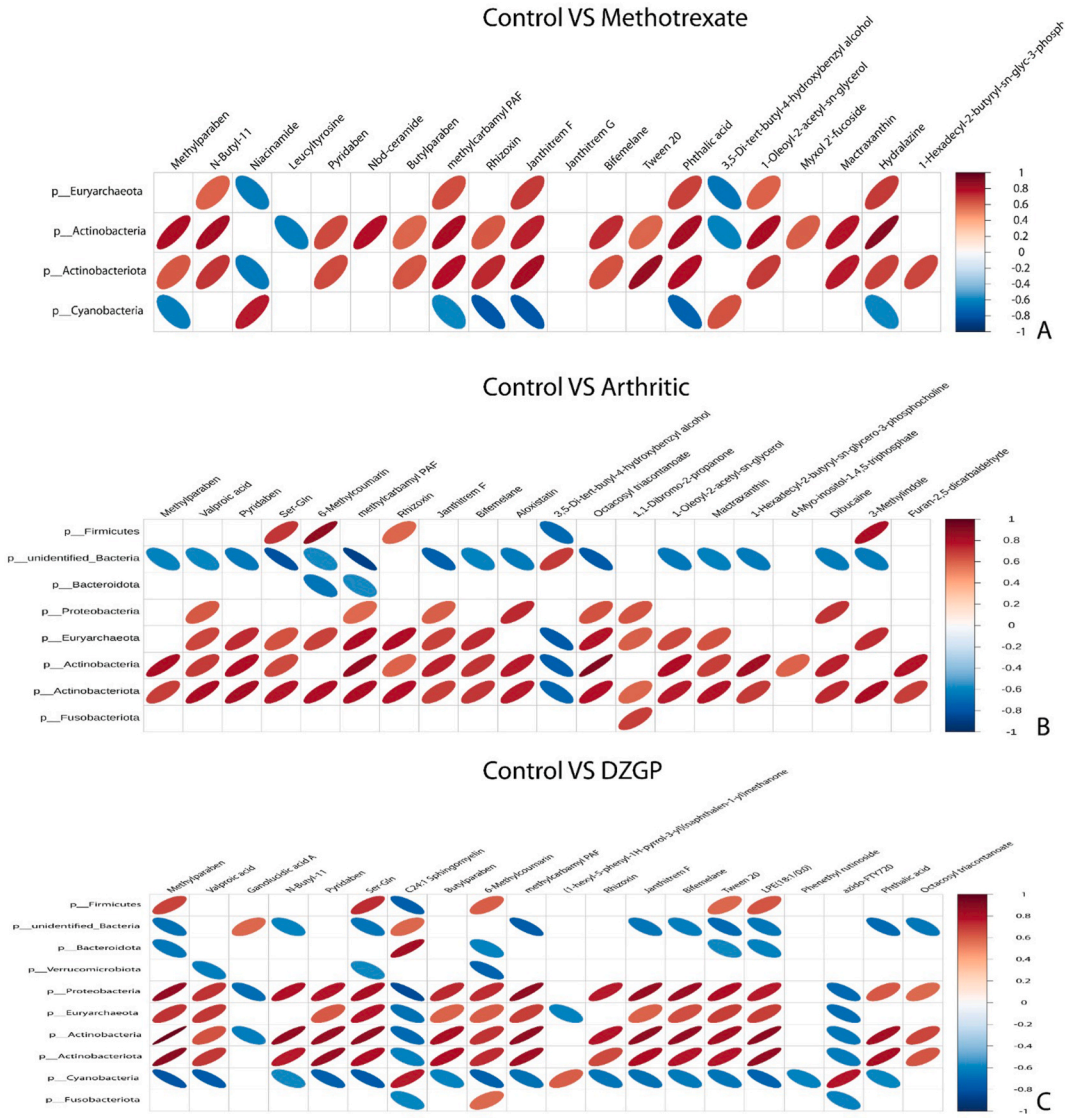

Fig. 10. Pearson correlation estimates between microbiome and top-20 abundant metabolites in control vs arthritic mice treated with commercially available Methotrexate drug (A), control vs RA mouse (B), and traditional Chinese medicine vs healthy control mice (C). The correlation bar is presented on right side of each panel. Maximum shift in microbial diversity at phylum level and correlation with metabolites was observed in case of DZGP treated mice.

5. Conclusions

The present study highlighted the beneficial aspect of Chinese traditional medicine (DZGP). The DZGP significantly altered the transcriptome of synovial fluid. Moreover, several metabolic changes were induced during treatment, which targeted the TNF-α and NF-κB signaling pathways, which are the main triggering factors in RA pathogenesis. The traditional treatment of DZGP led to promotion of beneficial gut microbiota and changes in metabolic pathways. The DZGP increased the abundance of Verrucomicrobiota and Cyanobacteria, which are well known bacterial phyla to promote gut health. Overall effects of DZGP resulted in recovery from RA by mediating inflammatory response through NF-κB signaling and promoting gut health.

Future Perspectives and limitations: In this study, we identified molecular pathways indicating that traditional Chinese medicines may affect the microbiome, transcriptome and metabolome in arthritic mouse. In the past, use of TCM was criticized due to absence of modern analytical research data of human body. Here, we provide the direct evidence of improvement in the disease treatment using a TCM. It is recommended that in the future, the knowledge gap of TCM use may be filled by integrated miciobiomics, transcriptomics and metabolomics data. Even though traditional drugs hold the great promise, but due to lack of supporting biological data, large numbers of people are reluctant to use them. Another limitation of the TCM is lack of biological data on humans. With the increasing omics data, it will be possible to tackle the limitations of TCM usage in China and other countries.

Ethical and consent statements

The study was conducted according to the guidelines for Animal Care and Use Committee of Sichuan University. The study was in complete compliance with the National Institutes of Health Guide for the Care and Use of Laboratory Animals and approved by Research Ethics Committee of Sichuan University (NO. SCU231124001).

Consent for publication

Not applicable.

Funding

This work was funded by The Open Fund of Hubei Key Laboratory of Biological Resources Protection and Utilization (Hubei Minzu University) (KYPT012302) and the National Natural Science Foundation of China (31971162, U20A20410 and 32071275).

Data availability statement

All data used in this manuscript are available within the text and its supplementary files.

Disclaimer/Publisher's note

The statements, opinions and data contained in all publications are solely those of the individual author(s) and contributor(s) and not of MDPI and/or the editor(s). MDPI and/or the editor(s) disclaim responsibility for any injury to people or property resulting from any ideas, methods, instructions or products referred to in the content.

CRediT authorship contribution statement

Liming Zhao: Writing – review & editing, Writing – original draft, Validation, Supervision, Resources, Project administration, Methodology, Investigation, Funding acquisition, Formal analysis, Data curation, Conceptualization. **Kai Zheng:** Writing – original draft, Methodology, Investigation, Formal analysis, Data curation, Conceptualization. **Xiaolin Wan:** Writing – original draft, Project administration, Methodology, Investigation, Formal analysis, Data curation, Conceptualization. **Qiang Xiao:** Writing – review & editing, Supervision, Software, Resources, Methodology, Formal analysis, Conceptualization. **Lin Yuan:** Writing – review & editing, Writing – original draft, Visualization, Supervision, Resources, Methodology, Conceptualization. **Chuanfang Wu:** Writing – review & editing, Writing – original draft, Resources, Funding acquisition, Formal analysis, Conceptualization. **Jinku Bao:** Writing – review & editing, Writing – original draft, Validation, Supervision, Project administration, Methodology, Data curation, Conceptualization.

Declaration of competing interest

The authors declare that they have no known competing financial interests or personal relationships that could have appeared to influence the work reported in this paper.

Acknowledgments

Not applicable.

Appendix A. Supplementary data

Supplementary data to this article can be found online at https://doi.org/10.1016/j.heliyon.2024.e33706.

References

[1] Y. Alamanos, A.A. Drosos, Epidemiology of adult rheumatoid arthritis, Autoimmun. Rev. 4 (2005) 130–136.
[2] D.M. Mitchell, P.W. Spitz, D.Y. Young, D.A. Bloch, D.J. McShane, J.F. Fries, Survival, prognosis, and causes of death in rheumatoid arthritis, Arthritis Rheum. Off. J. Am. Coll. Rheumatol. 29 (1986) 706–714.
[3] A.-C. Rat, M.-C. Boissier, Rheumatoid arthritis: direct and indirect costs. Jt, Bone Spine 71 (2004) 518–524.
[4] F. Matcham, I.C. Scott, L. Rayner, M. Hotopf, G.H. Kingsley, S. Norton, D.L. Scott, S. Steer, The impact of rheumatoid arthritis on quality-of-life assessed using the SF-36: a systematic review and meta-analysis, in: Proceedings of the Seminars in Arthritis and Rheumatism, Elsevier, 2014, pp. 123–130, vol. 44.
[5] D.P. Symmons, Mortality in rheumatoid arthritis, Br. J. Rheumatol. 27 (1988) 44–54.
[6] N.C.A. Horsten, J. Ursum, L.D. Roorda, D. van Schaardenburg, J. Dekker, A.F. Hoeksma, Prevalence of hand symptoms, impairments and activity limitations in rheumatoid arthritis in relation to disease duration, J. Rehabil. Med. 42 (2010) 916–921.
[7] S.M. Naz, D.P.M. Symmons, Mortality in established rheumatoid arthritis, Best Pract. Res. Clin. Rheumatol. 21 (2007) 871–883.

[8] S. Thierry, B. Fautrel, I. Lemelle, F. Guillemin, Prevalence and incidence of juvenile idiopathic arthritis: a systematic review. Jt, Bone Spine 81 (2014) 112–117.
[9] D. Symmons, Excess mortality in rheumatoid arthritis–is it the disease or the drugs? J. Rheumatol. 22 (1995) 2200–2202.
[10] J.S. Smolen, D. Aletaha, A. Barton, G.R. Burmester, P. Emery, G.S. Firestein, A. Kavanaugh, I.B. McInnes, D.H. Solomon, V. Strand, Rheumatoid arthritis, Nat. Rev. Dis. Prim. (2018) 418001.
[11] M.A.M. van Delft, T.W.J. Huizinga, An overview of autoantibodies in rheumatoid arthritis, J. Autoimmun. 110 (2020) 102392.
[12] I.A. Udalova, A. Mantovani, M. Feldmann, Macrophage heterogeneity in the context of rheumatoid arthritis, Nat. Rev. Rheumatol. 12 (2016) 472–485.
[13] M.D. Young, M.J. Wakefield, G.K. Smyth, A. Oshlack, Gene ontology analysis for RNA-seq: accounting for selection bias, Genome Biol. 11 (2010) 1–12.
[14] S. Alivernini, L. MacDonald, A. Elmesmari, S. Finlay, B. Tolusso, M.R. Gigante, L. Petricca, C. Di Mario, L. Bui, S. Perniola, Distinct synovial tissue macrophage subsets regulate inflammation and remission in rheumatoid arthritis, Nat. Med. 26 (2020) 1295–1306.
[15] M. Takahashi, T. Nishimura, K. Yokomuro, Quantitative analysis of cytokine gene expression in the liver, Immunol. Cell Biol. 77 (1999) 139–142.
[16] G. Yanni, M. Nabil, M.R. Farahat, R.N. Poston, G.S. Panayi, Intramuscular gold decreases cytokine expression and macrophage numbers in the rheumatoid synovial membrane, Ann. Rheum. Dis. 53 (1994) 315–322.
[17] J.J. Haringman, D.M. Gerlag, A.H. Zwinderman, T.J.M. Smeets, M.C. Kraan, D. Baeten, I.B. McInnes, B. Bresnihan, P.P. Tak, Synovial tissue macrophages: a sensitive biomarker for response to treatment in patients with rheumatoid arthritis, Ann. Rheum. Dis. 64 (2005) 834–838.
[18] S. Gay, R.E. Gay, W.J. Koopman, Molecular and cellular mechanisms of joint destruction in rheumatoid arthritis: two cellular mechanisms explain joint destruction? Ann. Rheum. Dis. 52 (1993) S39.
[19] S.E. Sweeney, G.S. Firestein, Rheumatoid arthritis: regulation of synovial inflammation, Int. J. Biochem. Cell Biol. 36 (2004) 372–378.
[20] Q.Y. Zeng, R. Chen, J. Darmawan, Z.Y. Xiao, S.B. Chen, R. Wigley, S. Le Chen, N.Z. Zhang, Rheumatic diseases in China, Arthritis Res. Ther. 10 (2008) 1–11.
[21] Q. Jia, L. Wang, X. Zhang, Y. Ding, H. Li, Y. Yang, A. Zhang, Y. Li, S. Lv, J. Zhang, Prevention and treatment of chronic heart failure through traditional Chinese medicine: role of the gut microbiota, Pharmacol. Res. 151 (2020) 104552.
[22] Y. He, A. Lu, Y. Zha, X. Yan, Y. Song, S. Zeng, W. Liu, W. Zhu, L. Su, X. Feng, Correlations between symptoms as assessed in traditional Chinese medicine (TCM) and ACR20 efficacy response: a comparison study in 396 patients with rheumatoid arthritis treated with TCM or western medicine, JCR J. Clin. Rheumatol. 13 (2007) 317–321.
[23] J. Fang, N. Zheng, Y. Wang, H. Cao, S. Sun, J. Dai, Q. Li, Y. Zhang, Understanding acupuncture based on ZHENG classification from system perspective, Evidence-Based Complement. Altern. Med. 2013 (2013).
[24] Y. Gong, Z. Yu, Y. Wang, Y. Xiong, Y. Zhou, C. Liao, Y. Li, Y. Luo, Y. Bai, B. Chen, Effect of moxibustion on HIF-1α and VEGF levels in patients with rheumatoid arthritis, Pain Res. Manag. 2019 (2019).
[25] J. Shan, L. Peng, W. Qian, T. Xie, A. Kang, B. Gao, L. Di, Integrated serum and fecal metabolomics study of collagen-induced arthritis rats and the therapeutic effects of the Zushima tablet, Front. Pharmacol. 9 (2018) 891.
[26] S. Abdollahi-Roodsaz, L.A.B. Joosten, M.I. Koenders, I. Devesa, M.F. Roelofs, T.R.D.J. Radstake, M. Heuvelmans-Jacobs, S. Akira, M.J.H. Nicklin, F. Ribeiro-Dias, Stimulation of TLR2 and TLR4 differentially skews the balance of T cells in a mouse model of arthritis, J. Clin. Invest. 118 (2008) 205–216.
[27] L. Wen, L. Shi, X.-L. Kong, K.-Y. Li, H. Li, D.-X. Jiang, F. Zhang, Z.-G. Zhou, Gut microbiota protected against Pseudomonas aeruginosa pneumonia via restoring treg/Th17 balance and metabolism, Front. Cell. Infect. Microbiol. 12 (2022) 856633.
[28] E. Gasteiger, C. Hoogland, A. Gattiker, S. Duvaud, M.R. Wilkins, R.D. Appel, A. Bairoch, Protein Identification and Analysis Tools on the ExPASy Server, Springer, 2005. ISBN 1588293432.
[29] K. Lewandowska, M. Szulc, A. Sionkowska, Effect of solvent on the hydrodynamic properties of collagen, Polymers 13 (2021) 3626.
[30] J. Luan, Z. Hu, J. Cheng, R. Zhang, P. Yang, H. Guo, G. Nan, N. Guo, X. Gou, Applicability and implementation of the collagen-induced arthritis mouse model, including protocols, Exp. Ther. Med. 22 (2021) 1–10.
[31] S. Seeuws, P. Jacques, J. Van Praet, M. Drennan, J. Coudenys, T. Decruy, E. Deschepper, L. Lepescheux, P. Pujuguet, L. Oste, A multiparameter approach to monitor disease activity in collagen-induced arthritis, Arthritis Res. Ther. 12 (2010) 1–10.
[32] Y. Liao, G.K. Smyth, W. Shi, FeatureCounts: an efficient general purpose program for assigning sequence reads to genomic features, Bioinformatics 30 (2014) 923–930.
[33] D. Risso, J. Ngai, T.P. Speed, S. Dudoit, Normalization of RNA-seq data using factor analysis of control genes or samples, Nat. Biotechnol. 32 (2014) 896–902.
[34] M.D. Robinson, D.J. McCarthy, G.K. Smyth, EdgeR: a bioconductor package for differential expression analysis of digital gene expression data, Bioinformatics 26 (2010) 139–140.
[35] R. Adusumilli, P. Mallick, Data conversion with ProteoWizard MsConvert, Proteomics methods Protoc (2017) 339–368.
[36] M. Kanehisa, M. Furumichi, M. Tanabe, Y. Sato, K. Morishima, KEGG: new Perspectives on Genomes, pathways, diseases and drugs, Nucleic Acids Res. 45 (2017) D353–D361.
[37] S. Mukhopadhyay, P. Aich, Cost effective method for GDNA isolation from the cecal content and high yield procedure for RNA isolation from the colonic tissue of mice, Bio-protocol 12 (2022).
[38] J. Shin, S. Lee, M.-J. Go, S.Y. Lee, S.C. Kim, C.-H. Lee, B.-K. Cho, Analysis of the mouse gut microbiome using full-length 16S RRNA amplicon sequencing, Sci. Rep. 6 (2016) 29681.
[39] A. Klindworth, E. Pruesse, T. Schweer, J. Peplies, C. Quast, M. Horn, F.O. Glöckner, Evaluation of general 16S ribosomal RNA gene PCR primers for classical and next-generation sequencing-based diversity studies, Nucleic Acids Res. 41 (2013).
[40] X. Zhang, M. Zhang, C.-T. Ho, X. Guo, Z. Wu, P. Weng, M. Yan, J. Cao, Metagenomics analysis of gut microbiota modulatory effect of green tea polyphenols by high fat diet-induced obesity mice model, J. Funct.Foods 46 (2018) 268–277.
[41] M. Lataretu, S. Krautwurst, A. Viehweger, C. Brandt, M. Hölzer, Targeted decontamination of sequencing data with CLEAN, bioRxiv (2023) 2008–2023.
[42] E. Bolyen, J.R. Rideout, M.R. Dillon, N.A. Bokulich, C.C. Abnet, G.A. Al-Ghalith, H. Alexander, E.J. Alm, M. Arumugam, F. Asnicar, Reproducible, interactive, scalable and extensible microbiome data science using QIIME 2, Nat. Biotechnol. 37 (2019) 852–857.
[43] A. Amir, D. McDonald, J.A. Navas-Molina, E. Kopylova, J.T. Morton, Z. Zech Xu, E.P. Kightley, L.R. Thompson, E.R. Hyde, A. Gonzalez, Deblur rapidly resolves single-nucleotide community sequence patterns, mSystems 2 (2017) 10–1128.
[44] B.D. Ondov, N.H. Bergman, A.M. Phillippy, Interactive metagenomic visualization in a web browser, BMC Bioinf. 12 (2011) 1–10.
[45] C. Lozupone, R. Knight, UniFrac: a new phylogenetic method for comparing microbial communities, Appl. Environ. Microbiol. 71 (2005) 8228–8235.
[46] R. McGraw, R. Zhang, Multivariate analysis of homogeneous nucleation rate measurements. Nucleation in the p-toluic acid/sulfuric acid/water system, J. Chem. Phys. 128 (2008).
[47] K. Lu, R.P. Abo, K.A. Schlieper, M.E. Graffam, S. Levine, J.S. Wishnok, J.A. Swenberg, S.R. Tannenbaum, J.G. Fox, Arsenic exposure perturbs the gut microbiome and its metabolic profile in mice: an integrated metagenomics and metabolomics analysis, Environ. Health Perspect. 122 (2014) 284–291.
[48] K. Wang, D. Zhang, Y. Liu, X. Wang, J. Zhao, T. Sun, T. Jin, B. Li, J.L. Pathak, Traditional Chinese medicine formula Bi-qi capsule alleviates rheumatoid arthritis-induced inflammation, synovial hyperplasia, and cartilage destruction in rats, Arthritis Res. Ther. 20 (2018) 1–12.
[49] I.B. McInnes, G. Schett, Cytokines in the pathogenesis of rheumatoid arthritis, Nat. Rev. Immunol. 7 (2007) 429–442.
[50] M.I. Vazquez, J. Catalan-Dibene, A.B. Zlotnik, Cells responses and cytokine production are regulated by their immune microenvironment, Cytokine 74 (2015) 318–326.
[51] N. Nishina, Y. Kaneko, H. Kameda, M. Kuwana, T. Takeuchi, Reduction of plasma IL-6 but not TNF-α by methotrexate in patients with early rheumatoid arthritis: a potential biomarker for radiographic progression, Clin. Rheumatol. 32 (2013) 1661–1666.
[52] P.P. Tak, G.S. Firestein, NF-KB: a Key role in inflammatory diseases, J. Clin. Invest. 107 (2001) 7–11.
[53] P.J. Barnes, M. Karin, Nuclear factor-κb—a pivotal transcription factor in chronic inflammatory diseases, N. Engl. J. Med. 336 (1997) 1066–1071.
[54] C.G. Shinde, M.P. Venkatesh, T.M.P. Kumar, H.G. Shivakumar, Methotrexate: a gold standard for treatment of rheumatoid arthritis, J. Pain Palliat. Care Pharmacother. 28 (2014) 351–358.

[55] R.S. Funk, R.K. Singh, M.L. Becker, Metabolomic profiling to identify molecular biomarkers of cellular response to methotrexate in vitro, Clin. Transl. Sci. 13 (2020) 137–146.
[56] H. Devarbhavi, M. Patil, V.V. Reddy, R. Singh, T. Joseph, D. Ganga, Drug-induced acute liver failure in children and adults: results of a single-centre study of 128 patients, Liver Int. 38 (2018) 1322–1329.
[57] J. Kim, Y. Kim, J. Choi, H. Jung, K. Lee, J. Kang, N. Park, Y.A. Rim, Y. Nam, J.H. Ju, Recapitulation of methotrexate hepatotoxicity with induced pluripotent stem cell-derived hepatocytes from patients with rheumatoid arthritis, Stem Cell Res. Ther. 9 (2018) 1–15.
[58] L. Luo, J. Zhang, M. Liu, S. Qiu, S. Yi, W. Yu, T. Liu, X. Huang, F. Ning, Monofloral triadica cochinchinensis honey polyphenols improve alcohol-induced liver disease by regulating the gut microbiota of mice, Front. Immunol. 12 (2021) 673903.
[59] C. Wang, S. Zhao, Y. Xu, W. Sun, Y. Feng, D. Liang, Y. Guan, Integrated microbiome and metabolome analysis reveals correlations between gut microbiota components and metabolic profiles in mice with methotrexate-induced hepatoxicity, Drug Des. Dev. Ther. (2022) 3877–3891.
[60] H.E. Rasmussen, I. Martínez, J.Y. Lee, J. Walter, Alteration of the gastrointestinal microbiota of mice by edible blue-green algae, J. Appl. Microbiol. 107 (2009) 1108–1118.
[61] F. Lindenberg, L. Krych, J. Fielden, W. Kot, H. Frøkiær, G. Van Galen, D.S. Nielsen, A.K. Hansen, Expression of immune regulatory genes correlate with the abundance of specific clostridiales and verrucomicrobia species in the equine ileum and cecum, Sci. Rep. 9 (2019) 12674.
[62] L.H. Orellana, T. Ben Francis, M. Ferraro, J.-H. Hehemann, B.M. Fuchs, R.I. Amann, Verrucomicrobiota are specialist consumers of sulfated methyl pentoses during diatom blooms, ISME J. 16 (2022) 630–641.